A method for construction of second-order accuracy difference schemes permitting no false two-grid-interval wave in the height field

By FEDOR MESINGER, *Department of Meteorology, University of Belgrade, Yugoslavia*

(Manuscript received August 7, 1972; revised version April 16, 1973)

ABSTRACT

A method has been developed to inherently prevent the false two-grid-interval wave in height field, which is, to the author's knowledge, at present permitted as a stationary solution to the gravity-wave part of all space-centered schemes used to solve the primitive equations in numerical forecasting and simulation experiments. The proposed method preserves space- and time-centered differencing and second-order accuracy. It involves introduction of auxiliary velocity points midway between the neighboring height grid points. Velocity components at these auxiliary points are assumed to have space-averaged values at the beginning of a considered time step; acceleration contributions are evaluated and added to these initial values to obtain components at the middle or at the end of the time step. Resulting velocity components are then used for a more accurate calculation of the divergence term in the continuity equation. The procedure leads to schemes which propagate single-grid-point height perturbations to all the existing height grid points, and thus do not permit formation of a false high wave number noise in the forecast fields. For the Heun, leapfrog, and implicit time differencing schemes an analysis is performed of the effect that this procedure has on the properties of the scheme. For the Heun scheme, the procedure results in a reduction of the instability of the scheme, and in a reduction of the truncation error. For the leapfrog scheme slight instability is produced; however, values of the amplification factors, and a numerical example, indicate that this modified leapfrog scheme can still successfully be used for integration of the primitive equations. For the implicit scheme, the procedure preserves the unconditional stability of the scheme, and also reduces the truncation error. Finally, a numerical example is shown, giving a dramatic illustration of the advantages of the proposed method.

1. Problem and proposed method

For an analysis of the problem, consider the two-dimensional linearized shallow-water equations

$$\frac{\partial u}{\partial t} + g\frac{\partial h}{\partial x} = 0, \quad \frac{\partial v}{\partial t} + g\frac{\partial h}{\partial y} = 0,$$
$$\frac{\partial h}{\partial t} + H\nabla \cdot \mathbf{v} = 0 \tag{1}$$

The symbols here have their usual meaning. We note that the solution of (1) are gravity waves which propagate with a constant phase speed $\sqrt{gH}$. Further, we will have in mind that the terms in (1) can be regarded as representing only a part of the complete system of the primitive equations.

We now want to look at some aspects of the situation created when the space derivatives in (1) are substituted by their straightforward space-centered finite difference analogues. For that we need a decision on the space arrangement of dependent variables. We restrict there our considerations to the three rectangular arrangements shown in Fig. 1. The identifying letters (A), (E) and (C) are chosen so as to conform with a study by Winninghoff & Arakawa (Arakawa, 1972). For three considered types of lattice the same standard space-centered difference operators δ_x and δ_y can be used for our purpose, so that the system (1) is replaced by

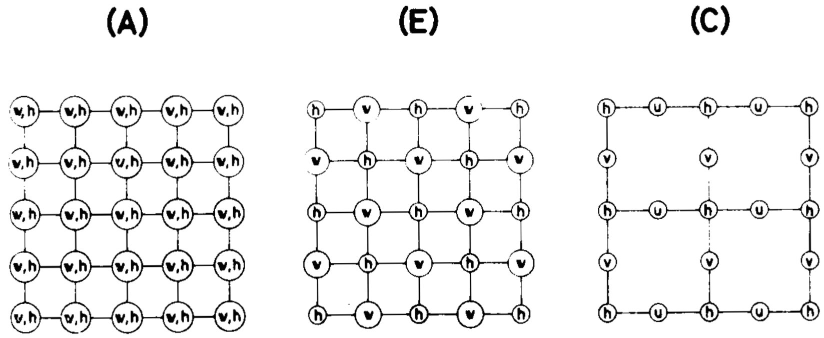

Fig. 1. Three types of lattice considered for the finite difference solution of (1).

$$\frac{\partial u}{\partial t} + g\delta_x h = 0, \quad \frac{\partial v}{\partial t} + g\delta_y h = 0,$$
$$\frac{\partial h}{\partial t} + H(\delta_x u + \delta_y v) = 0 \qquad (2)$$

Here, for example,

$$\delta_x h(x, y) \equiv \frac{1}{2d^*}[h(x + d^*, y) - h(x - d^*, y)]$$

where, if the grid distance d is always the shortest distance between positions of the same variables, d^* is equal to d, $d/\sqrt{2}$, and $d/2$, for the lattice (A), (E), and (C), respectively.

With the same value of d^*, as on Fig. 1, the truncation error of (2) will be the same. Yet, the lattice (E) will have two times, and the lattice (C) four times less variables per unit area than the lattice (A); accordingly, they will require that much less computing time. Unfortunately, the lattice (C) is not convenient when the Coriolis force terms are present in the equations; see for example, the referred study by Winninghoff & Arakawa (Arakawa, 1972, p. 45). It has never been used for extensive numerical integrations of the complete system of the primitive equations.

Resorting, then, to the lattice (E), we want to analyze the effect of finite space differences in (2) on the solution of the system. Substituting

$$\begin{pmatrix} u \\ v \\ h \end{pmatrix} \equiv \mathrm{Re}\left[\begin{pmatrix} u_0 \\ v_0 \\ h_0 \end{pmatrix} e^{i(kx + ly - \nu t)}\right] \qquad (3)$$

as a trial solution of (2), we find that the ratio of the phase speed $c = \nu/\sqrt{k^2 + l^2}$ to the true phase speed $\sqrt{gH}$ is given by

$$\frac{c}{\sqrt{gH}} = \sqrt{\frac{\sin^2 X + \sin^2 Y}{X^2 + Y^2}}, \qquad (4)$$

where

$$X \equiv kd/\sqrt{2}, \quad Y \equiv ld/\sqrt{2}.$$

The waves admitted by the lattice (E) cover a triangular region on the wave-number plane k, l. The values of the relative phase speed (4), on half of that triangular region, are shown in Fig. 2. The remaining half of the triangular region is left out to avoid duplication, since (4) is symmetric with respect to the line $l = k$. One can observe a general decrease in the relative phase speed with an increase in the wave number. Most disturbingly, a neutral and stationary two-grid-interval wave is permitted as a solution of the system (2), as shown by the zero phase speed value at the right corner of the

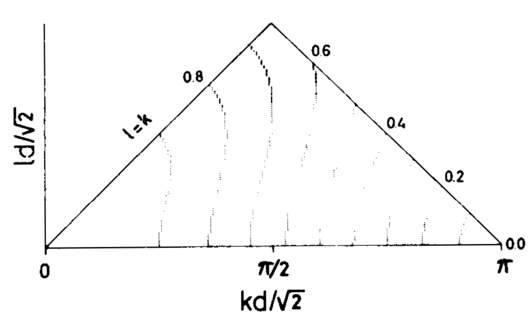

Fig. 2. Relative phase speed of gravity waves, as a function of wave numbers k and l, in case when the space derivatives in (1) are substituted by their straightforward space-centered finite difference analogues.

diagram. Examination of (2) shows that this false solution can have an arbitrary amplitude in all three of the dependent variables.

For an understanding of this phenomenon, notice that the lattice (E) can be viewed as being formed by a superposition of two (C) lattices, shifted diagonally for the distance $\sqrt{2}d^*$ with respect to each other. Solutions of the system (2) on each of these two subsets of variables have no possibility of interacting with each other. In particular, constant values at one subset of variables is a stationary solution on that subset, no matter what values have variables of the other subset. Two stationary solutions, with different constants on each of the two subsets, will be viewed as a false stationary two-grid-interval wave when the two subsets of variables are considered simultaneously. This wave will form a stationary striped pattern. With a complete system of primitive equations, excitation of gravity waves is possible inside the computational region. If a disturbance is then excited so as to involve variables of one subset only, it will propagate as a gravity wave so as to stay confined to that subset of variables; the other subset will be affected only through much slower Coriolis and advection terms. In this way propagating waves will also appear as short wave, approximately two-grid-interval, noise in the forecast. As an extreme example, suppose (2) had a source term for height, and was being applied to the problem in which the water was being poured at one of the height grid points. The four height points nearest to it would never be affected by that action, although physically they should be the first to notice it.

In the same way the (A) lattice can be considered as being formed by a superposition of two (E) lattices. Thus, it will contain four independent gravity waves, each propagating on a separate subset of variables. They may produce a noisy pattern when viewed simultaneously.

This "two-grid-interval wave" problem can become a serious inconvenience when gravity waves of significant amplitude are excited by forcing terms and/or boundary conditions. Occasionally a clear separation of solutions occurs; see, for example, some figures in a report by Gerrity & McPherson (1970). In addition, as shown by Gerrity (1972), an excessive amplitude of the two grid-interval wave may be the cause of a nonlinear instability of the computation.

As possible remedial measures, filtering (Gerrity & McPherson, 1970), or damping of the small scale features of the divergent part of the flow only (Sadourny, 1972), have been recommended. An obvious alternative to filtering or damping the short waves that are falsely generated by independent propagation of gravity waves on two subsets of variables, is to try designing a scheme which would be free of this false generation of short waves. One scheme having this property, as demonstrated by Arakawa (1972), is obtained using time-alternating space-uncentered differencing. It eliminates the possibility of the false two-grid-interval wave in all of the variables. The method has a first-order accuracy. It is being used by Arakawa in combination with the Matsuno time-uncentered differencing, also of the first-order accuracy.

Examination of the terms in (1), however, shows that a velocity perturbation can propagate as a gravity wave only through excitation of height perturbations, and vice versa. Thus, it need not be necessary to prevent the false two-grid-interval wave in both the height and the velocity fields: elimination of one of them should suffice to prevent the formation of the other. It is, therefore, believed of interest to point out a possibility to inherently prevent the false two-grid-interval noise in the height field, and at the same time preserve space- and time-centered differencing and second-order accuracy. Fortuitously, an emphasis on the prevention of the height noise, as compared to that on the prevention of the velocity noise, or of both simultaneously, is also the alternative justified by the forcing terms of the complete system of the primitive equations. Of these terms, heating generates space disturbances in the height field, while friction tends to smooth out the space noise in the velocity field.

To arrive at the underlying idea, consider any two neighboring height points within the lattice (E). A height perturbation at one of these points is not able to affect the other point because of no velocity at the midpoint between the two; this velocity is needed to bring about the height change at the other point through the divergence term in the continuity equation. To circumvent this difficulty one can introduce auxiliary velocity points midway between the height points. There is no need to carry any variables at these auxiliary points; velocity components there can be assumed to have space-averaged values at the beginning of a considered time step, and acceleration contributions can then be evaluated and added to these initial values to obtain components at the middle or at the end of the time step. Resulting velocity components can then be used for a more accurate calculation of the divergence term in the continuity equation. This procedure leads to schemes in which single-grid-point height perturbations are propagated through gravity waves to all the existing height grid points, thus inherently permitting no false space-noise in the height field. These schemes will be referred to in the sequel as AM (Acceleration-Modified) schemes.

The proposed procedure will be illustrated for the case of the Heun scheme, followed by an analysis of the effect that it has on the accuracy, stability, and phase speed of the waves. The resulting finite difference equations, and the results of the accuracy, stability and phase speed analysis, will then also be given for the leapfrog and the implicit time differencing scheme. Finally, results of a numerical test will be shown.

2. The Heun and the AM-Heun scheme

Among the three considered schemes the Heun scheme (see, for example, Haltiner, 1971) has a structure which is most similar to that of the proposed modification procedure. Hence, it will be used for a more detailed illustration and analysis of the method. Having linear equations, the same scheme is obtained if we have a first forward and a time-averaged second step, or if we perform the time centering by ending the forward step at the middle of the time step. We choose the latter alternative. We also find it convenient to have $2\Delta t$ represent the time step of the Heun scheme; this makes the total number of evaluations of the time derivatives equal to the total number of time increments Δt elapsed. Centering the time index at the middle of the $2\Delta t$ time step, Heun time differencing then transforms (2) into

$$\begin{aligned} u^{\tau+1} &= u^{\tau-1} - 2g\Delta t\,\delta_x h^{\tau-1} \\ &\quad + 2gH(\Delta t)^2\,\delta_x(\delta_x u + \delta_y v)^{\tau-1}, \\ v^{\tau+1} &= v^{\tau-1} - 2g\Delta t\,\delta_y h^{\tau-1} \\ &\quad + 2gH(\Delta t)^2\,\delta_y(\delta_x u + \delta_y v)^{\tau-1}, \\ h^{\tau+1} &= h^{\tau-1} - 2H\Delta t(\delta_x u + \delta_y v)^{\tau-1} \\ &\quad + 2gH(\Delta t)^2\,\nabla_+^2 h^{\tau-1} \end{aligned} \tag{5}$$

Here superscripts denote the time level of the variables, and, if double subscripts are used to denote a repeated application of the δ operator,

$$\nabla_+^2 h \equiv (\delta_{xx} + \delta_{yy})h \tag{6}$$

The expression (6) is readily recognized as the standard five-point finite difference Laplacian; its subscript indicates directions along which it is computed.

Now consider the following modification of this procedure. At regular velocity points, as before,

$$u^\tau = u^{\tau-1} - g\Delta t\,\delta_x h^{\tau-1}, \quad v^\tau = v^{\tau-1} - g\Delta t\,\delta_y h^{\tau-1}$$

In addition, auxiliary velocity points are introduced midway between the height points, as shown by circled numbers 5, 6, 7 and 8 in Fig. 3. At these points accelerations along lines joining the neighboring height points will be evaluated, to enable interaction between neighboring height values through propagation of gravity waves. As for the velocity components themselves, it will suffice to assume that at the beginning of the time step they have their space-avaraged values. Only components u' at points 5 and 7, and v' at points 6 and 8 are needed, the orientation of the system x', y' being as shown in Fig. 3. Therefore,

$$u'^{\tau-1} = \frac{\sqrt{2}}{2}(\bar{u}^{y'} + \bar{v}^{y'})^{\tau-1}, \quad v'^{\tau-1} = \frac{\sqrt{2}}{2}(-\bar{u}^{x'} + \bar{v}^{x'})^{\tau-1}$$

where a superior bar denotes a two-point average taken along the direction indicated following the bar sign. To these initial values acceleration contributions are added to obtain values at the middle of the $2\Delta t$ time step, that is,

$$u'^\tau = u'^{\tau-1} - g\Delta t\,\delta_{x'} h^{\tau-1}, \quad v'^\tau = v'^{\tau-1} - g\Delta t\,\delta_{y'} h^{\tau-1}$$

The velocity divergence in (1) at time level τ can now be approximated by

$$\tfrac{1}{2}(\delta_x u + \delta_y v)^\tau + \tfrac{1}{2}(\delta_{x'} u' + \delta_{y'} v')^\tau$$

thereby giving equal weight to all eight directions of the lattice. With other steps done in the conventional way, one obtains a system which differs from (5) only by having the height equation take the form

$$h^{\tau+1} = h^{\tau-1} - 2H\Delta t(\delta_x u + \delta_y v)^{\tau-1} + 2gH(\Delta t)^2 \nabla^2_{\bigcirc} h^{\tau-1} \tag{7}$$

where

$$\nabla^2_{\bigcirc} h \equiv \frac{1}{4d^2}[h_1 + h_2 + h_3 + h_4 + 2(h_5 + h_6 + h_7 + h_8) - 12h_0] \tag{8}$$

is a nine-point finite difference Laplacian. The subscript of the Laplacian (8) again indicates directions along which it is computed; the expression on the right side is readily obtained when the approximation to Laplacian is derived by giving equal weight to all directions of the stencil in Fig. 3. Thus, the AM-Heun scheme differs from the conventional Heun scheme (5) only in that the nine-point Laplacian (8) has replaced the five-point Laplacian (6) in the third equation. This allows for propagation of gravity waves along all height points of the grid, thus admitting no false space noise in the height field.

Accuracy. We shall compare the accuracy of the two schemes. If the truncation error is defined as in Richtmyer & Morton (1967, p. 20), one obtains for the conventional Heun scheme

$$\varepsilon_h = \tfrac{1}{12} H(u_{xxx} + v_{yyy}) d^2 - \tfrac{2}{3} H(u_x + v_y)_{tt} (\Delta t)^2 + \tfrac{1}{12} H(u_{xxx} + v_{yyy})_t d^2 \Delta t + \tfrac{1}{3} H(u_x + v_y)_{ttt} (\Delta t)^3 + \dots \tag{9}$$

where ε_h is the truncation error of the third of Eqs. (5). For the AM-Heun scheme, the only difference in second and third-order terms of ε_h appears in that the $d^2\Delta t$ term takes the form

$$\tfrac{1}{24} H(u'_{x'x'x'} + v'_{y'y'y'})_t d^2 \Delta t \tag{10}$$

Thus, compared to the conventional Heun scheme, the AM-Heun scheme preserves the second-order accuracy, and, moreover, results in some reduction of the truncation error.

Stability and phase speed analysis. For a linear stability and phase speed analysis of the two schemes, consider the trial solution

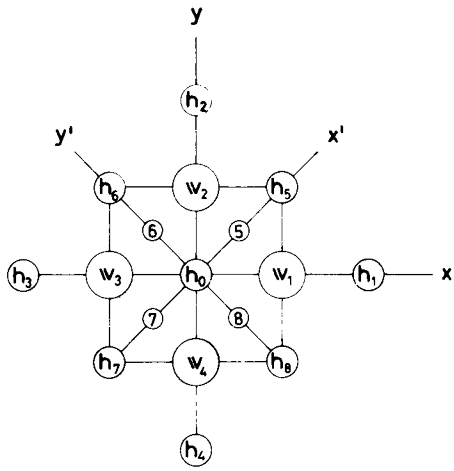

Fig. 3. Stencil used to describe the construction of proposed schemes, and for definitions of Laplacians (8) and (22).

$$\begin{pmatrix} u^\tau \\ v^\tau \\ h^\tau \end{pmatrix} \equiv \mathrm{Re}\left[\begin{pmatrix} u_0 \\ v_0 \\ h_0 \end{pmatrix} \lambda^\tau e^{i(kx+ly)}\right] \tag{11}$$

where

$$\lambda \equiv |\lambda| e^{-i\nu\Delta t} \tag{12}$$

Substitution of (11) into (5) leads to the homogeneous system

$$\begin{aligned} &(\lambda^2 - 1 + 4gH\mu^2 \sin^2 X) u_0 + 4gH\mu^2 \sin X \sin Y v_0 + i2\sqrt{2} g\mu \sin X h_0 = 0, \\ &4gH\mu^2 \sin X \sin Y u_0 + (\lambda^2 - 1 + 4gH\mu^2 \sin^2 Y) v_0 + i2\sqrt{2} g\mu \sin Y h_0 = 0, \\ &i2\sqrt{2} H\mu \sin X u_0 + i2\sqrt{2} H\mu \sin Y v_0 + [\lambda^2 - 1 + 4gH\mu^2(\sin^2 X + \sin^2 Y)] h_0 = 0 \end{aligned} \tag{13}$$

where $\mu \equiv \Delta t/d$.

For the AM-Heun scheme, the only difference is that instead of the expression within the square bracket of (13) one obtains

$$\lambda^2 - 1 + 4gH\mu^2[\sin^2 X + \sin^2 Y + \tfrac{1}{2}(\cos X - \cos Y)^2] \tag{14}$$

Requirement for the determinants of considered systems to vanish gives, for each scheme, three solutions for λ^2. One is, for both schemes,

$$\lambda^2 = 1 \tag{15}$$

The remaining two are

$$\lambda^2 = 1 - 4A \pm 2\sqrt{-2A} \tag{16}$$

for the conventional Heun scheme, and

$$\lambda^2 = 1 - 4A - B \pm \sqrt{B^2 - 8A} \tag{17}$$

for the AM-Heun scheme; in these expressions

$$A = gH\mu^2(\sin^2 X + \sin^2 Y),$$

$$B = gH\mu^2(\cos X - \cos Y)^2$$

In view of the definition of λ, (15) is seen to represent a neutral and stationary solution. (Since computation is done in time steps of $2\Delta t$, the non-stationary solution $\lambda = -1$ is of no meaning.) It is instructive to analyze this stationary solution in some detail. We can distinguish a number of cases:

Case I: $\sin X$ and $\sin Y$ are both different from zero. From (13) we then obtain

$$\sin X\, u_0 + \sin Y\, v_0 = 0,$$

$$h_0 = 0$$

This can readily be verified as satisfying $\delta_x u + \delta_y v = 0$, a sufficient requirement, in addition to $h_0 = 0$, to have in (5) all the terms containing Δt equal to zero.

Case II: one of $\sin X$ and $\sin Y$ is equal to zero, and the other is not. Then one of the amplitudes u_0 and v_0 can have an arbitrary value, while the other must be zero. Also, $h_0 = 0$. This is the case of a translational motion along one of the axes of the grid, with an arbitrary wave number in that velocity component, except 0 and $\sqrt{2}\pi/d$, along the other axis.

Case III: $\sin X$ and $\sin Y$ are both equal to zero. Then, for the conventional Heun scheme, arbitrary amplitudes u_0, v_0 and h_0 are allowed. u, v and h are either constants (when both k and l are zero); or they have a striped pattern (when one of k and l is equal to $\sqrt{2}\pi/d$ and the other is zero). Thus, a neutral and stationary two-grid-interval wave is allowed in all of the variables.

For the AM-Heun scheme, with the square bracket of (13) replaced by (14), arbitrary amplitude h_0 is allowed only when $\cos X = \cos Y$. This can happen only when $k = l = 0$, that is, when h is constant. When one of k and l is equal to $\sqrt{2}\pi/d$ we have $\cos X \neq \cos Y$, and h_0 must be zero. Thus, the neutral and stationary two-grid-interval wave is allowed in u and v fields, but not in the height field.

We turn now to the solutions (16) and (17), that are not identically neutral. For the conventional Heun scheme (16) gives

$$|\lambda| = \sqrt{1 + 16A^2}$$

This scheme is, thus, amplifying at all admissible points of the wave-number plane except at those where $A = 0$ (constant fields or a two-grid-interval wave), when it is neutral. Instability is most intensive at the point $X = Y = \pi/2$.

Amplification factor of the AM-Heun scheme is identical to that of the conventional scheme when $B = 0$. This happens on the line $l = k$, and includes the point of maximum instability of the conventional scheme. Otherwise, two cases can be distinguished:

Case I: $B^2 - 8A \leq 0$. The difference between absolute values of the right sides of (16) and (17) is then equal to $2B(1 - 4A)$. Thus, we see that the modification reduces the instability of the Heun scheme when $4A < 1$. This is a somewhat stronger condition than the Courant-Friedrichs-Lewy (CFL) stability criterion $\sqrt{2A} \leq 1$ (see the leapfrog scheme analysis in the next section). To satisfy $4A < 1$ time step has to be less than $1/\sqrt{2}$ of the time step needed to satisfy the CFL criterion. However, when using the Heun scheme time step had anyway to be chosen even substantially less than the one needed for $4A < 1$, in order that the instability be kept at an acceptably low level. In this way, the modification reduces the instability of the scheme.

Case II: $B^2 - 8A > 0$. With acceptable choices of time step this happens only in relatively small regions next to the points $A = 0$, $B > 0$. The AM-Heun scheme is then stable and damping.

As an illustration of possible values of the amplification factors of the two schemes, Fig. 4 shows the values of $|\lambda|$ obtained using (16) and (17), and with $2\sqrt{gH}\mu$ (maximum value of $\sqrt{2A}$) equal to 0.25. Again, the values of $|\lambda|$ are sym-

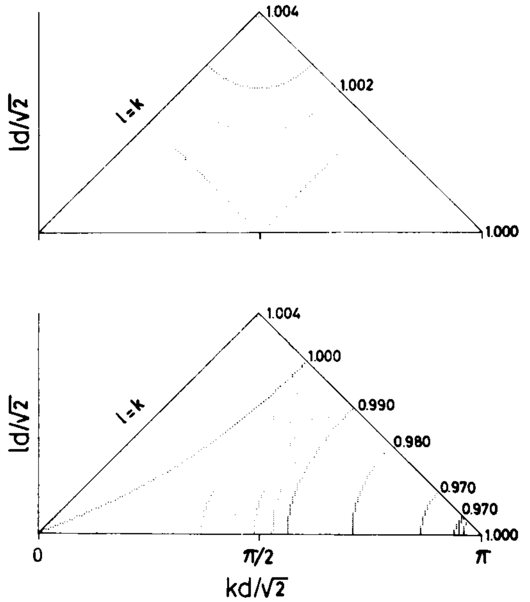

Fig. 4. Amplification factor of gravity waves, as a function of wave numbers k and l, in cases when the conventional Heun scheme (upper diagram), and when the "acceleration-modified" Heun scheme (lower diagram) are used for the finite difference solution of (1).

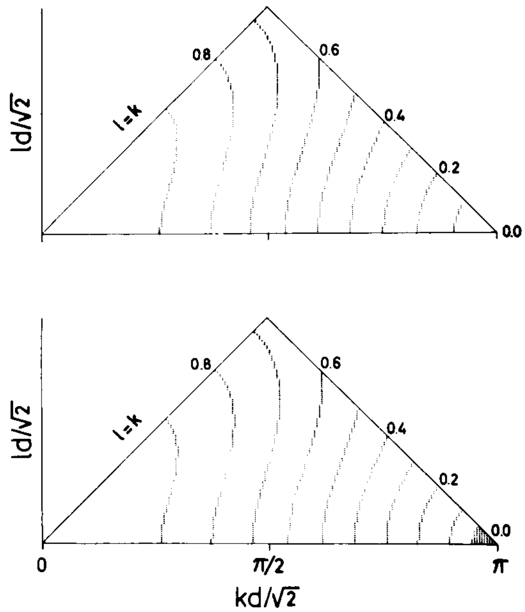

Fig. 5. Relative phase speed of gravity waves, as a function of wave numbers k and l, in cases when the conventional Heun scheme (upper diagram), and when the "acceleration-modified" Heun scheme (lower diagram) are used for the finite difference solution of (1).

metric with respect to the line $l=k$; and, to avoid repetition, the diagrams are terminated at that line. In the region where the AM-Heun scheme has two values of $|\lambda|$ of the non-neutral solution, next to the right corner of the lower diagram, isolines are printed to describe the greater of the two values. A fairly intensive damping of the shortest close-to-two-grid-interval waves is seen in the lower AM-Heun scheme diagram. Due to the modification of the scheme, instability is seen to have been reduced to a region of the wave-number plane centered along the line $l=k$. For considered gravity-wave terms, however, one must expect the usefulness of the scheme to still remain limited to rather short integrations or an intermittent use only. If a longer integration with an explicit two-level scheme is desired, one could for these terms use a stable AM scheme obtained by an analogous modification of the Matsuno scheme (Matsuno, 1966), or of a scheme intermediate to those of Heun and Matsuno (Mesinger, 1972).

It is of interest to also consider the phase speed of the non-neutral solutions, as compared to the true phase speed $\sqrt{gH}$. Using (12) and (16) we obtain, for the conventional Heun scheme,

$$\frac{c}{\sqrt{gH}} = \frac{1}{2\mu\sqrt{2gH(X^2+Y^2)}} \arctan\left(\mp\frac{2\sqrt{2A}}{1-4A}\right) \tag{18}$$

For the AM-Heun scheme, using (17), we obtain

$$\frac{c}{\sqrt{gH}} = \frac{1}{2\mu\sqrt{2gH(X^2+Y^2)}} \arctan\left(\mp\frac{\sqrt{8A-B^2}}{1-4A-B}\right),$$

$$\text{when } B^2-8A \leqslant 0 \tag{19 a}$$

and

$$\frac{c}{\sqrt{gH}} = 0, \quad \text{when } B^2-8A>0 \tag{19 b}$$

From (18) and (19) we see that in (16) and (17) the upper and lower signs correspond to the computational and to the physical mode, respectively.

The relative phase speeds (18) and (19), with signs of the physical mode, and with values of the constant $2\sqrt{gH}\mu$ as used for the preceding figure, are shown in Fig. 5. As before, to avoid repetition, the diagrams are terminated at the line $l=k$. The upper diagram, when compared to that shown in Fig. 2, illustrates the accelerating property of the conventional Heun differencing. The phase speed error is seen to be reduced, compared to that due to space differencing only, at all except two corner points of the diagram. As to the difference between the two diagrams in Fig. 5, the most notable one is the appearance of a small region of zero phase speed next to the right corner of the lower diagram. Since the solution of the AM-Heun scheme in that region is damped, there is no danger that it can be excited to a significant amplitude. Otherwise, the isolines of the two diagrams are very similar. Only a careful comparison reveals that, except in and next to the corner region and on the line $l=k$, some increase in the phase speed has occurred as a result of the modification of the scheme.

3. The leapfrog and the AM-leapfrog scheme

When the conventional leapfrog scheme is used for the system (2), there results the finite difference system

$$u^{\tau+1} = u^{\tau-1} - 2g\Delta t\,\delta_x h^\tau,$$

$$v^{\tau+1} = v^{\tau-1} - 2g\Delta t\,\delta_y h^\tau,$$

$$h^{\tau+1} = h^{\tau-1} - 2H\Delta t(\delta_x u + \delta_y v)^\tau \tag{20}$$

It permits no gravity wave propagation between the neighboring height points of the lattice (E).

The remedial modification, as described in Section 1, requires a two-step or an implicit scheme constructing procedure; therefore, it can not be applied in form of the regular one-step and explicit leapfrog differencing. However, one can use the regular leapfrog differencing for the first two equations and for half of the velocity divergence in (1), calculated along the axes x, y of the stencil in Fig. 3, and a first-forward-then-centered procedure for the remaining half of that velocity divergence, calculated along the axes x', y' of the considered stencil. For the first forward step now height fields of two time levels are available; thus, one can take a weighted average of the height variables of the two levels. In this way (1) is replaced by a scheme which differs from (20) only by having the height equation take the form

$$h^{\tau+1} = h^{\tau-1} - H\Delta t[(\delta_x u + \delta_y v)^\tau + (\delta_x u + \delta_y v)^{\tau-1}] + gH(\Delta t)^2[b\nabla_{\mathrm{x}}^2 h^\tau + (1-b)\nabla_{\mathrm{x}}^2 h^{\tau-1}] \tag{21}$$

where

$$\nabla_{\mathrm{x}}^2 h \equiv \frac{1}{d^2}(h_5 + h_6 + h_7 + h_8 - 4h_0) \tag{22}$$

is a five-point finite difference Laplacian, calculated along directions indicated by its subscript, and b is a constant. The choice of $b=0$ makes the modification procedure take the form of the Heun scheme, and the choice $b=1/2$ makes the first forward step of that procedure centered in time. In any case, the modification again allows for propagation of gravity waves along all height points of the grid.

Accuracy. An analysis analogous to that of the preceding section gives as the truncation error of the third of the equations of the conventional leapfrog scheme

$$\varepsilon_h = \tfrac{1}{12}H(u_{xxx} + v_{yyy})d^2 - \tfrac{1}{6}H(u_x + v_y)_{tt}(\Delta t)^2 + \text{terms of the } \textit{fourth} \text{ and higher order.} \tag{23}$$

For the AM-leapfrog scheme (21) gives as the truncation error

$$\varepsilon_h = \tfrac{1}{12}H(u_{xxx} + v_{yyy})d^2 + [\tfrac{1}{12} - \tfrac{1}{2}(1-b)]H(u_x + v_y)_{tt}(\Delta t)^2 \tag{24}$$
$$+ \text{terms of the } \textit{third} \text{ and higher order.}$$

Thus, compared to the conventional scheme, the AM-leapfrog scheme again preserves the second-order accuracy. Its truncation error attains a minimum value for $b=5/6$, when the $(\Delta t)^2$ term in (24) vanishes. Thus, we see that the constant b can be chosen so as to make the AM-leapfrog scheme more accurate than the conventional scheme. With the time-centered first step of the modification procedure, that is, with $b=1/2$, there is no change in the second-order terms. The only difference in the truncation error of the two schemes then is that some third-order terms have appeared in the error of the AM-scheme.

Stability and phase speed analysis. Substitution of (11) into equations of the conventional leapfrog scheme (20) gives

$$(\lambda^2 - 1)u_0 + i\lambda 2\sqrt{2}\,g\mu \sin X\, h_0 = 0,$$

$$(\lambda^2 - 1)v_0 + i\lambda 2\sqrt{2}\,g\mu \sin Y\, h_0 = 0, \qquad (25)$$

$$i\lambda 2\sqrt{2}\,H\mu \sin X\, u_0 + i\lambda 2\sqrt{2}\,H\mu \sin Y\, v_0 + (\lambda^2 - 1)h_0 = 0$$

For the AM-leapfrog scheme, instead of the third equation of (25) one obtains

$$i(\lambda+1)\sqrt{2}\,H\mu \sin X\, u_0 + i(\lambda+1)\sqrt{2}\,H\mu \sin Y\, v_0 + [\lambda^2 - 1 + (b\lambda + 1 - b)4gH\mu^2(1 - \cos X \cos Y)] \times h_0 = 0 \qquad (26)$$

Requirement for the determinants of considered systems to vanish gives now, for each scheme, six solutions for λ. Two are, for both schemes,

$$\lambda = 1 \qquad (27)$$

and

$$\lambda = -1 \qquad (28)$$

For the conventional leapfrog scheme, the four remaining solutions are given by

$$\lambda^2 = 1 - 4A \pm 2\sqrt{2A(2A-1)} \qquad (29)$$

For the AM-leapfrog scheme, one of the four solutions is a duplication of the temporal computational mode (28). The three solutions that still remain are given by

$$(\lambda+1)(\lambda-1)^2 + 4(b\lambda + 1 - b)(\lambda - 1)C + 4\lambda A = 0 \qquad (30)$$

where $C = gH\mu^2(1 - \cos X \cos Y)$.

Now, a detailed analysis and comparison of all admissible solutions can be carried out in the manner of the preceding section. As the point of most interest here, in case of the conventional leapfrog scheme the neutral and stationary solution (27) includes the two-grid-interval wave in all of the variables. For the AM scheme, however, again the neutral and stationary

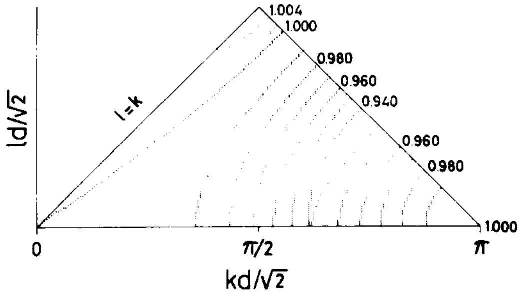

Fig. 6. Amplification factor of gravity waves, as a function of wave numbers k and l, in case when the "acceleration-modified" leapfrog scheme is used for the finite difference solution of (1).

two-grid-interval wave is allowed only in u and v fields, and not in the height field.

For stability of the two schemes behavior of solutions given by (29) and (30), that are not unconditionally neutral, has to be investigated. For the conventional leapfrog scheme, (29) shows that the well-known CFL stability criterion is with present notation obtained as a requirement that

$$\sqrt{2A} \leq 1$$

be satisfied for all the admissible waves. When this is true, all solutions are neutral, and the scheme is stable. For the AM-leapfrog scheme, amplification factors given by the three roots of (30) have to be analyzed. To this end maximum values of these three amplification factors were printed as a function of k and l, for a number of values of the parameter b. Isolines describing the numerical values of these amplification factors, obtained with $b = 1/2$ and $2\sqrt{gH}\mu$ equal to 0.50, are shown in Fig. 6. Some instability can be noticed, centered along the line $l = k$ of the wave-number plane. If the value of the parameter b is decreased with respect to the value $b = 1/2$, this instability along the line $l = k$ increases. If, on the other hand, the value of the parameter b is increased beyond the value $b = 1/2$, an unstable region appears at the right corner of the diagram, showing that unstable two-grid-interval waves become permitted. In this way one is led to a conclusion that the best stability properties of the AM-leapfrog scheme are obtained with the choice $b = 1/2$, as used for the values shown in Fig. 6.

This appearance of an instability in case of the leapfrog scheme limits, of course, the useful-

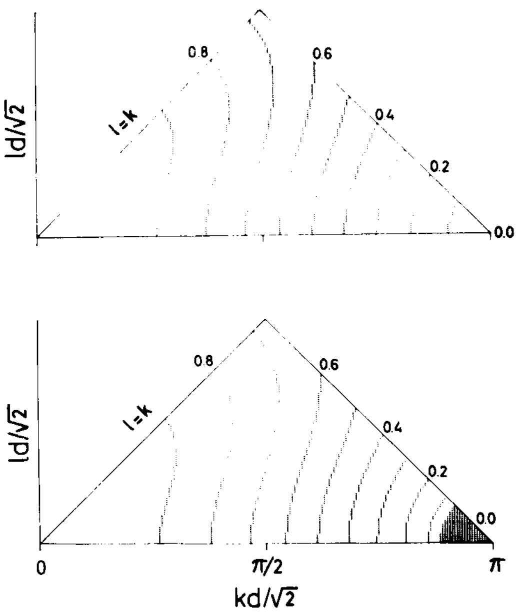

Fig. 7. Relative phase speed of gravity waves, as a function of wave numbers k and l, in cases when the conventional leapfrog scheme (upper diagram), and when the "acceleration-modified" leapfrog scheme (lower diagram) are used for the finite difference solution of (1).

ness of the proposed modification procedure. For longer integrations with the leapfrog scheme, one may either use the AM scheme only intermittently, or, since the amplification is not large, one may attempt to find and use a time step short enough as to reduce the instability to a degree which can be controlled by the physical dissipation present in the complete system of the primitive equations. A successful numerical test of the AM-leapfrog scheme with $2\sqrt{gH}\mu$ equal to 0.71 and no physical dissipation terms, will be shown in Section 5.

For the relative phase speed, using (29) one obtains, when $2A \leqslant 1$,

$$\frac{c}{\sqrt{gH}} = \frac{1}{2\mu\sqrt{2gH(X^2+Y^2)}} \times \text{arc tan}\left(\mp\frac{2\sqrt{2A(1-2A)}}{1-4A}\right) \quad (31)$$

Here again the lower sign is seen to refer to the physical mode. For the AM-leapfrog scheme, relative phase speed of the physical mode has to be obtained from (30); it appears of little use to describe it with explicit formulas here. Fig. 7 shows numerical values of (31), with the sign of the physical mode, and those of the relative phase speed of the physical mode of (30); both are computed with $2\sqrt{gH}\mu$ as used for the preceding figure. The upper diagram illustrates the property of the conventional leapfrog differencing of also having an accelerating effect. The phase error is seen to be reduced by just about the same amount as in the example shown for the Heun differencing, in the upper diagram of Fig. 5. As to the difference between the two diagrams in Fig. 7, the most notable one is again the appearance of a small region of zero phase speed next to the right corner of the AM scheme diagram. Compared to the Heun scheme diagrams, some increase in the area of this zero phase speed region can now be noticed. Otherwise, again as in the case of the Heun scheme, a careful comparison of the two diagrams reveals that a slight reduction in the phase speed error has occurred over most of the diagram as a result of the modification of the scheme.

4. The implicit and the AM-implicit scheme

When an implicit scheme is used for the system (1) it is again convenient to have $2\Delta t$ represent the time step of the scheme. Namely, with a more complete system of equations it will be practical to evaluate the additional terms at the middle of the time step used for the implicit differencing of the terms in (1), as suggested by Kwizak & Robert (1971). The differencing procedure then has to be repeated at time increments of half of the time step used for the implicit differencing; that is, at time increments Δt if the time step of implicit differencing is defined to be $2\Delta t$. With that definition, and centering the time index at the middle of the $2\Delta t$ time step, implicit time differencing transforms (2) into a system that can be written in the form

$$\begin{aligned} u^{\tau+1} &= u^{\tau-1} - g\Delta t\delta_x(h^{\tau-1}+h^{\tau+1}), \\ v^{\tau+1} &= v^{\tau-1} - g\Delta t\delta_y(h^{\tau-1}+h^{\tau+1}), \qquad (32) \\ h^{\tau+1} &= h^{\tau-1} - 2H\Delta t(\delta_x u + \delta_y v)^{\tau-1} \\ &\quad + gH(\Delta t)^2\nabla_+^2(h^{\tau-1}+h^{\tau+1}) \end{aligned}$$

This system again permits no gravity wave propagation between the neighboring height points of the lattice (E).

The modification described in Section 1 can here be applied in a straightforward manner. One performs the regular implicit differencing for the first two equations and for half of the velocity divergence in the third equation of (1). The remaining half of that velocity divergence is calculated along the axes x', y' of the stencil in Fig. 3, using velocity components at auxiliary velocity points. These components are computed by space averaging at the beginning of the $2\Delta t$ time step; acceleration contributions are then evaluated by implicit time differencing and added to the initial values to obtain components at the end of the $2\Delta t$ time step. The considered second half of the velocity divergence is then approximated using an arithmetic average of the values for the beginning and for the end of that time step. In this way (1) is replaced by a scheme which differs from (32) only by having the height equation take the form

$$h^{\tau+1} = h^{\tau-1} - 2H\Delta t(\delta_x u + \delta_y v)^{\tau-1} + gH(\Delta t)^2 \nabla^2_{\bigcirc}(h^{\tau-1} + h^{\tau+1}) \quad (33)$$

Thus, as in case of the Heun differencing, with the implicit differencing again the AM scheme differs from the conventional scheme only in that the nine-point Laplacian (8) has replaced the five-point Laplacian (6) in the third equation. As before, this allows for propagation of gravity waves along all height points of the grid.

Accuracy. As the truncation error of the third of the equations of the conventional implicit scheme one obtains

$$\varepsilon_h = \tfrac{1}{12}H(u_{xxx} + v_{yyy})d^2 + \tfrac{1}{3}H(u_x + v_y)_{tt}(\Delta t)^2 + \tfrac{1}{12}H(u_{xxx} + v_{yyy})_t d^2 \Delta t + \tfrac{1}{3}H(u_x + v_y)_{ttt}(\Delta t)^3 + \dots \quad (34)$$

For the modified scheme, again as in case of the Heun differencing, the only difference in second and third order terms of ε_h appears in that the $d^2\Delta t$ term takes the form

$$\tfrac{1}{24}H(u'_{x'x'x'} + v'_{y'y'y'})_t d^2 \Delta t \quad (35)$$

Thus, compared to the conventional scheme, the AM-implicit scheme again preserves the second-order accuracy, and results in some reduction of the truncation error.

Stability and phase speed analysis. Substitution of (11) into equations of the conventional implicit scheme (32) gives

$$\begin{aligned}
&(\lambda^2 - 1)u_0 + i(\lambda^2+1)\sqrt{2}\,g\mu \sin X\, h_0 = 0,\\
&(\lambda^2 - 1)v_0 + i(\lambda^2+1)\sqrt{2}\,g\mu \sin Y\, h_0 = 0, \quad (36)\\
&i2\sqrt{2}\,H\mu \sin X\, u_0 + i2\sqrt{2}\,H\mu \sin Y\, v_0 \\
&\quad + [\lambda^2 - 1 + (\lambda^2+1)\,2gH\mu^2(\sin^2 X + \sin^2 Y)]h_0 = 0
\end{aligned}$$

For the AM-implicit scheme, the only difference is that instead of the expression within the square bracket of (36) one obtains

$$\lambda^2 - 1 + (\lambda^2 + 1)\,2gH\mu^2 \times [\sin^2 X + \sin^2 Y + \tfrac{1}{2}(\cos X - \cos Y)^2] \quad (37)$$

Requirement for the determinants of considered systems to vanish gives, for each scheme, three solutions for λ^2. One is, for both schemes,

$$\lambda^2 = 1 \quad (38)$$

The remaining two are

$$\lambda^2 = \frac{1}{1+2A}(1 - 2A \pm 2\sqrt{-2A}) \quad (39)$$

for the conventional implicit scheme, and

$$\lambda^2 = \frac{1}{1+2A+B}(1 - 2A \pm \sqrt{B^2 - 8A}) \quad (40)$$

for the AM-implicit scheme.

Analysis of (36) shows that, as before, in case of the conventional scheme the neutral and stationary solution $\lambda = 1$ includes the two-grid-interval wave in all of the variables. For the AM scheme the neutral and stationary two-grid-interval wave is again allowed only in u and v fields, and not in the height field.

The temporal computational mode $\lambda = -1$ results from defining as $2\Delta t$ the time step of the scheme. Namely, when the differencing procedure is then repeated at time increments Δt, there exist, as far as the terms in (1) are concerned, two decoupled solutions.

For stability of the two schemes amplification factors given by (39) and (40) have to be

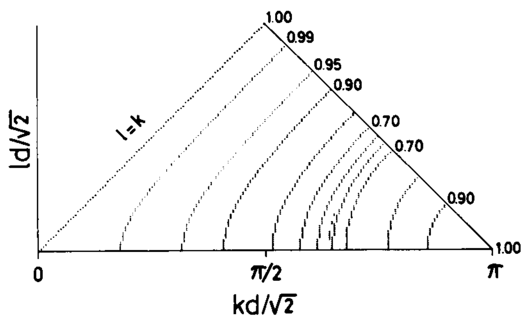

Fig. 8. Amplification factor of gravity waves, as a function of wave numbers k and l, in case when the "acceleration-modified" implicit scheme is used for the finite difference solution of (1).

analyzed. Using (39) one readily demonstrates the well-known property of the conventional implicit scheme of being unconditionally neutral. An analysis of (40) shows that the AM-implicit scheme is damping at all admissible points of the wave-number plane except at those where either $A = 0$ (constant fields or a two-grid-interval wave) or $B = 0$ (on the line $l = k$), when it is neutral. Thus, the modification preserves the unconditional stability of the implicit differencing scheme.

Isolines giving an example of the numerical values of the amplification factors given by (40) are shown in Fig. 8. They are obtained using for the constant $2\sqrt{gH}\mu$ the value of 2.5. In the region where (40) gives two different values of $|\lambda|$, again the greater of the two values is shown in the figure. The intensity of damping of the short four- to two-grid-interval waves, if computed per unit time, is seen to be very similar to that of the leapfrog scheme with five times shorter time steps, shown in Fig. 6.

For the relative phase speed, using (39) one obtains

$$\frac{c}{\sqrt{gH}} = \frac{1}{2\mu\sqrt{2gH(X^2+Y^2)}} \arctan\left(\mp\frac{2\sqrt{2A}}{1-2A}\right) \tag{41}$$

For the AM-implicit scheme, using (40), one obtains

$$\frac{c}{\sqrt{gH}} = \frac{1}{2\mu\sqrt{2gH(X^2+Y^2)}} \arctan\left(\mp\frac{\sqrt{8A-B^2}}{1-2A}\right),$$

$$\text{when } B^2 - 8A \leqslant 0 \tag{42 a}$$

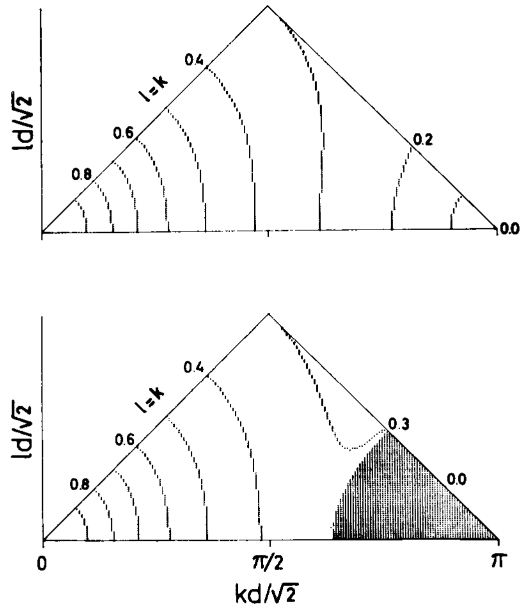

Fig. 9. Relative phase speed of gravity waves, as a function of wave numbers k and l, in cases when the conventional implicit scheme (upper diagram), and when the "acceleration-modified" implicit scheme (lower diagram) are used for the finite difference solution of (1).

and

$$\frac{c}{\sqrt{gH}} = 0, \quad \text{when } B^2 - 8A > 0 \tag{42 b}$$

As before, the lower signs are seen to refer to the physical model.

The relative phase speeds (41) and (42), with signs of the physical mode, and with $2\sqrt{gH}\mu$ as used for the preceding figure, are shown in Fig. 9. Its upper diagram illustrates the property of the conventional implicit differencing of having a decelerating effect. As to the lower diagram, as its most notable feature we notice that the zone of zero phase speed occupies now a fairly large area. This is due to a rather long time step used. The impression given by this zero phase speed zone may, however, be to some extent deceiving. Namely, when approaching this zone from the side of longer waves the phase speed of the physical mode, with constants as in the figure, approaches to a positive value such as to just produce no local phase changes in values taken at time increments Δt. With further decrease in wave

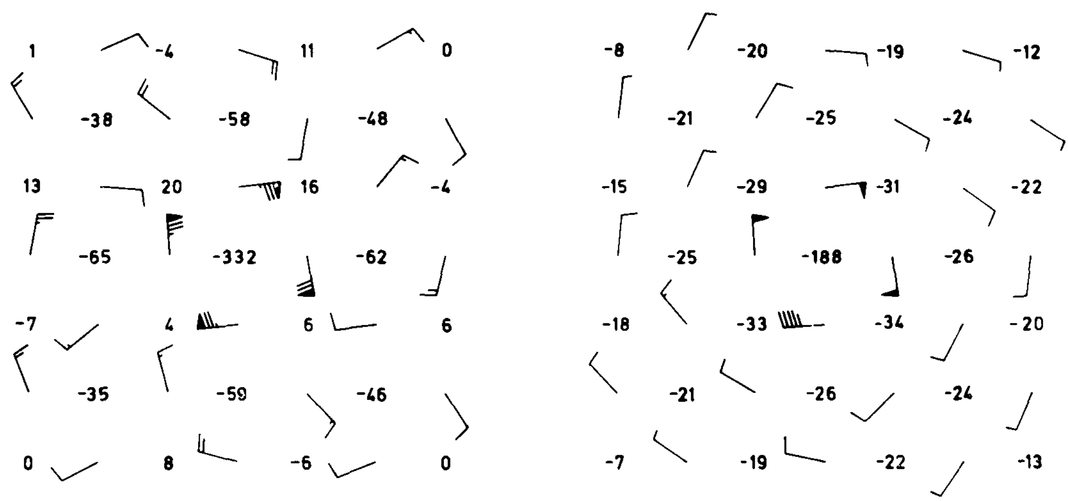

Fig. 10. Results of an integration made using the conventional leapfrog scheme (left half), and using the "acceleration modified" leapfrog scheme (right half of the figure). The figure shows the height and wind fields around a point mass sink of constant intensity.

length this phase speed can be considered to stay positive and change in such a way as to have the local phase changes taken at increments Δt remain zero; that is, to have

$$\frac{c}{\sqrt{gH}} = \mp \frac{\pi}{2\mu\sqrt{2gH(X^2+Y^2)}}$$

instead of zero in (42*b*). In that case there would be no discontinuity and no zero phase speed values inside the AM scheme diagram of Fig. 9. Otherwise, a careful comparison of the two phase speeds shows that, as before, a slight reduction in the phase speed error has occurred over most of the diagram as a result of the modification of the scheme.

5. A numerical example

A numerical test has been made, designed so as to illustrate the advantages of the proposed method in a very dramatic way. It is a duplication of examples given by Winninghoff and Arakawa (Arakawa, 1972): starting with a fluid at rest and with a constant free surface height, a point mass source and a point mass sink are prescribed, 10 grid intervals apart. Shallow water equations are then integrated, including the advection and the Coriolis terms, but no physical dissipation terms. One integration was here performed using the conventional leapfrog scheme, and space-centered differencing, always over two grid intervals ($2d^*$ in the notation of Section 1). Another integration was performed different only in that the AM-leapfrog scheme was used for the divergence term of the continuity equation. The AM-leapfrog scheme terms due to the nonlinear and Coriolis terms, not present in (1) and (21), are easily obtained with the help of the divergence equation. Namely, instead of following the procedure of preceding sections, the divergence equation can be used to evaluate the local change in velocity divergence from the beginning to the middle or the end of the time step. In case of leapfrog scheme this readily leads to (21) (the value $b = 1/2$ was used here), with a number of additional terms.

Results of the two integrations, in a square region around the sink point and at 21 hour time, are shown in Fig. 10. The left half of the figure shows the height and wind fields obtained using the conventional leapfrog scheme, and the right half those obtained using the AM-leapfrog scheme. The numbers show the height of the free surface, in meters, when the initial value of 1 000 m is subtracted. The wind fields are shown following the usual synoptic practice, except that the speed is indicated to within 1 m sec^{-1} accuracy, with each full-length barb standing for 5 m sec^{-1}. The integrations were performed on a region of 28×18 grid intervals, with constant height and no-slip boundary conditions. The source and sink had a constant intensity of 2 m $\min^{-1}$, and the Coriolis parameter was taken to be 10^{-4} $\sec^{-1}$. The initial step was done with the Heun and the AM-Heun scheme. Time steps of 15 minutes were used, with $d = 250$ km; this made the constant $2\sqrt{gH}\mu$ equal to 0.71.

The figure shows a striking difference between the two integrations. The conventional leapfrog scheme is seen to have produced a striped pattern in the height field, with false secondary circulations neighboring the main vortex around the sink point. The AM scheme gave a monotonic slope of the free surface toward the sink point, and a rather smooth vortex around it. No sign of instability of this AM integration has been noticed.

In case of stratified flow, heat sources and sinks would have an effect on the geopotential height field same as the mass sources and sinks have on the free surface height in the present experiments.

6. Conclusion

It has proven feasible to modify the Heun, leapfrog and the implicit differencing schemes for the gravity wave terms of the primitive equations in such a way as to retain the second-order accuracy in both space and time, and yet eliminate the possibility of a false neutral and stationary two-grid-interval wave in the height field. The modification procedure makes a single-grid-point height perturbation propagate as a gravity wave along all height points of the grid. Since a velocity perturbation can propagate as a gravity wave only through excitation of height perturbations, the method is believed sufficient to prevent the false two-grid-interval noise in all of the dependent variables. Along with a method of Arakawa, this is, as far as known to the author, the only method proposed so far that enables propagation of gravity waves along all points of a grid convenient in geophysical fluid dynamics. However, the present method has an accuracy one order higher, both in space and time, than the method of Arakawa. Thus, its use in numerical models is expected to improve the simulation of forcing processes occurring on a smaller horizontal scale. For example, the method could enable a more adequate simulation of the response of the atmosphere to sharp mountains and small scale heating, such as the heating due to condensation occurring in narrow bands and single-grid-point clouds.

Acknowledgements

It is a pleasure to acknowledge the benefit that the author had from several discussions with Prof. Akio Arakawa, of the Department of Meteorology, University of California, Los Angeles. The author also wishes to thank Mr. Zaviša Janjić, for making the programs used to print the isolines of the amplification factor and phase speed figures; and Mr. Zaviša Janjić and Miss Desanka Vukasović, both of the Center for the Atmospheric Sciences, University of Belgrade, for programing and carrying out the numerical test of Section 5.

REFERENCES

Arakawa, A. 1972. Design of the UCLA general circulation model. Dept. of Meteorology, University of California, Los Angeles, Numerical Simulation of Weather and Climate, Tech. Rept. No. 7, 116 pp.

Gerrity, J. P., Jr. 1972. A note on the computational stability of the two-step Lax-Wendroff form of the advection equation. *Mon. Wea. Rev. 100*, 72–73.

Gerrity, J. P., Jr. & McPherson, R. D. 1970. Noise analysis of a limited-area fine-mesh prediction model. Weather Bureau, Suitland, Md., ESSA Tech. Memo. WBTM NMC 46, 81 pp.

Haltiner, G. J. 1971. *Numerical weather prediction.* Wiley, New York. 317 pp.

Kwizak, M. & Robert, A. J. 1971. A semi-implicit scheme for grid point atmospheric models of the primitive equations. *Mon. Wea. Rev. 99*, 32–36.

Matsuno, T. 1966. Numerical integrations of the primitive equations by a simulated backward difference method. *J. Meteor. Soc. Japan*, Ser. 2, *44*, 76–84.

Mesinger, F. 1972. Computation of the wind by forced adjustment to the height field. *J. Appl. Meteor. 11*, 60–71.

Richtmyer, R. D. & Morton, K. W. 1967. *Difference methods for initial value problems.* Wiley, New York. 405 pp.

Sadourny, R. 1972. Conservative finite difference approximation of the primitive equations on quasi-uniform spherical grids. Central Analysis Office, Montreal, GARP RCPG on Computational Considerations, Third Progress Report, 17–18.

МЕТОД ПОСТРОЕНИЯ РАЗНОСТНОЙ СХЕМЫ ВТОРОГО ПОРЯДКА ТОЧНОСТИ, СВОБОДНЫЙ ОТ ЛОЖНОЙ ДВУХИНТЕРВАЛЬНОЙ ВОЛНЫ В ПОЛЕ БЫСОТЫИЗОБАРИЧЕСКОЙ ПОВЕРХНОСТИ

Развивается метод, предотвращающий возникновение ложной двухинтервальной волны в поле высоты, которая, насколько известно автору, присутствует в гравитационно-волновой части всех центрально-разностных по пространству схем, используемых для решения примитивных уравнений в численном прогнозе и в экспериментах по моделированию. Предложенный метод сохраняет центральные разности по времени и по пространству и втотой порядок точности. Он использует вспомогательные точки для вычисления скорости посередине между точками для вычисления высоты.

Предполагается, что компоненты скорости в этих вспомогательных точках сглажены по пространству в начале рассматриваемого интервала времени; вычисляется вклад ускорений, который добавляется к этим начальным значениям для получения скоростей в середине и конце шага по времени. Получившиеся компоненты скорости далее используются для более точного вычисления дивергенции в уравнении неразрывности. Процедура приводит к схеме, которая добавляет только одноточечные возмущения ко всем существующим узлам для вычисления высоты, и, таким образом, не позволяет формироваться ложным возмущениям с большими волновыми числами в прогностических полях. Оценивается эффект, который эта процедура оказывает на разностные схемы Хена, центральных разностей и неявную. Для схемы Хена процедура дает уменьшение неустойчивости и ошибки аппроксимации. В схеме центральных разностей появляется слабая неустойчивость, однако множитель возрастания и численный пример указывают, что эта модифицированная схема все еще может с успехом использоваться для интегрирования примитивных уравнений. Для неявной схемы процедура сохраняет безусловную устойчивость и уменьшает ошибку аппроксимации. Наконец, продемонстрирован численный пример со впечатляющей иллюстрацией преимуществ предложенного метода.